Long Report for Experiment on the Hall Effect

Candidate no. 265095
December 2023

Declaration

This long report is to be graded as part of the Physics Years 2 Laboratory module.

I declare that this report is entirely my own work, and that where supporting information has been drawn from other sources, those sources are fully and properly cited.

I am aware of the checklist of frequent errors made in Long Reports, which has been made available to me via Canvas. I understand that if I fail to check my work adequately against that list I am liable to make simple mistakes that could potentially result in a substantial reduction in marks. Word count of 3165.

Abstract

The aim of this experiment was to measure the Hall coefficient for a doped InSb wafer at both room temperature and at the boiling point of Nitrogen. The Hall coefficient was determined by placing the wafer in a known magnetic field of (159 ± 5)mT, varying the current from 1.1mA to 45.0mA. The Hall voltage and standard voltage across the wafer were recorded in both directions perpendicular to the magnetic field. The two measured Hall voltages were combined to eliminate the voltage drop due to the wafer's internal resistance. This combined Hall voltage was used to determine the wafer's Hall coefficient at both 291K and 77K.

Temperature K	Hall Coefficient R_H	Reduced χ^2
291	$-(3.1 \pm 0.1) \times 10^{-4}$	0.044
77	$(2.13 \pm 0.07) \times 10^{-2}$	0.048

Table 1: Hall coefficient result for InSb at 293K and 77K.

Contents

1 Introduction

The primary aim of this experiment was to determine the Hall coefficient, R_H, for a piece of semiconducting wafer. The wafer was a doped sample of Indium Antimonide. In industry, the importance of the Hall effect is supported by the need to determine accurately carrier density, electrical resistivity, and the mobility of carriers in semiconductors.[2]

Measuring the induced Hall voltage with the wafer immersed in liquid Nitrogen allows R_H to be determined at a known exact temperature of 77K. In this way, different semiconductors and doping techniques can be compared by quantifying their R_H. R_H was also measured at room temperature to see how the charge carrier sign, number and mobility change with temperature.

The Hall effect has major real-world applications in the usage of Hall effect sensors. These sensors are commonly integrated circuits that amplify the Hall voltage to measure the strength of a corresponding magnetic field. These can be used as proximity, speed and position sensors; highly valued in automation, manufacturing and motor industries.[3]

2 Theory

2.1 Band Theory in Semiconductors

In order to understand the properties of the semiconductor that was investigated, it was important to outline the concept of band theory, which provides a way of understanding the electronic properties of materials such as insulators, conductors and semiconductors.

Band theory categorises electrons into two distinct bands within a material; a valence and a conductor band. In the valence band, electrons are locked in place, unable to move and carry charge. The conduction band is where electrons are de-localised from their atomic structure, and are free to move in the material and carry charge. A majority of chemical bonding can be explain by atoms wanting to fill their outer shell of electrons, as this corresponds to their lowest energy state. The chemical bonding of a material therefore determines whether electrons exist in the valence or conductive band and whether they can move between these two bands.

This band analogy explains the conductivity of metals where atoms are bonded to one another in a lattice structure with a sea of de-localised electrons that are free to carry charge. It also explains why covalent and ionic bonded compounds are usually good insulators, as in these bonds, electrons donated or shared and thus bound to their respective nuclei. They neither significantly influence, nor are influenced by, an electric field.

Semiconductors sit between these two extremes and are commonly made from metalloid elements such as Silicon, Gallium or Indium, which are positioned between metals and non-metals on the periodic table. The properties of these semiconductors can be further altered through the introduction of impurities,

called doping. This is where different elements are forced into the present atomic structure and either contribute electrons or induce a deficit, referred to as an electron 'hole'. The type of doping is referred to as either 'n' or 'p' for positive and negatively respectively, depending on the overall effect. It's worth noting the electron hole can also move freely, and so acts as a positive quasi-particle, capable of carrying charge. This is shown visually in Figure 2.1.

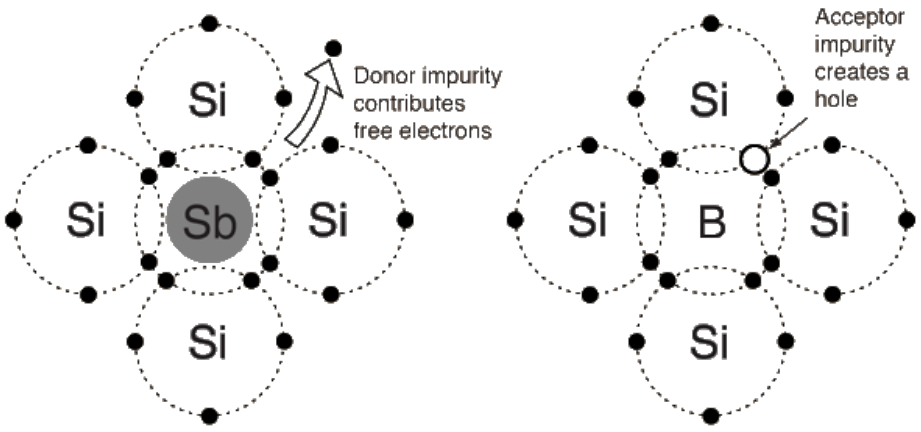

Figure 2.1: The atomic structure for an example p and n doped silicon semiconductor. Here, Antimony donates an electron to the structure and creates a n-type semiconductor. Boron creates an electron and so creates a p-type semiconductor. Source:`https://hyperphysics.phy-astr.gsu.edu/hbase/Solids/dope.html`

Doping does not change the band gap between the valence and conduction bands. It does, however, influence the Fermi level, which corresponds to the density of available conducting electrons within a material. Whilst both forms of doping generally increase the number of available charge carriers, the type of doping indicates whether these charge carriers are electrons or holes.

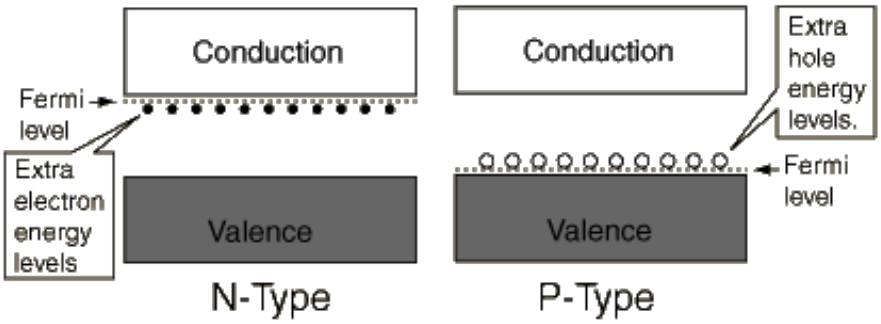

Figure 2.2: A visual comparison of the band gaps of n-type and p-type semiconductors. In particular, the difference in Fermi levels. Source: `https://hyperphysics.phy-astr.gsu.edu/hbase/Solids/dsem.html`

Temperature also plays a vital role in chemical bonding and as such, also in the mobility of electrons to move between the two bands. Metals are typically saturated with charge carriers with their valence and conduction bands overlapping. Therefore increasing the temperature causes those charge carriers to oscillate more violently, disrupting the overall flow of charge and increasing resistance. Semiconductors do not have an excess of charge carriers so generally resistance decreases with temperature. This is because more charge carriers are thermally excited to move from the valence to the conduction band, enabling more charge to flow.

2.2 Hall Effect

The Hall effect was first discovered by Edwin Hall in 1879, he was greatly influenced by the publication of the Maxwell equations. At that time, the newly found relationships between the electric and magnetic fields were being explored experimentally. He found that a magnetic field influences the motion of charge carriers already moving within an electric field. This is due to the Lorentz force,

$$\mathbf{F} = q(\mathbf{E} + \mathbf{v} \times \mathbf{B}), \tag{2.2.1}$$

acting upon individual charge carriers, where q is the charge of the charge carrier, $\mathbf{E}$ is the electric field, $\mathbf{v}$ is the velocity of the charge carrier, and $\mathbf{B}$ is the magnetic field.

The quantity, n, and respective charge, q, of the charge carriers present within a material is given by the Hall coefficient,

$$R_H = \frac{1}{nq}. \tag{2.2.2}$$

This is a material property, a magnetic field causes both charge carriers of either positive or negative charge to move in the same direction. Therefore, in

semiconductors, it is defined by both positive (holes) and negative (electrons) charge carriers;

$$R_H = \frac{n_h\mu_h^2 - n_e\mu_e^2}{e(n_h\mu_h + n_e\mu_e)^2}, \tag{2.2.3}$$

where n is charge carrier density and μ is charge carrier mobility, with those quantities for holes and electrons denoted by the subscripts $_h$ and $_e$ respectively. $e \approx 1.602 \times 10^{-19}$C is simply the fundamental charge. Substituting $b = \frac{\mu_e}{\mu_h}$ the ratio of electron to hole mobility, gives a simpler expression,

$$R_H = \frac{p - nb^2}{e(p + nb)^2} \tag{2.2.4}$$

The Hall coefficient represents the reciprocal of the number of charge carriers (and their sign) within a specific volume. It therefore has units of $\frac{\mathrm{m}^3}{\mathrm{C}}$. It's therefore clear to see how R_H is related to the doping of the semiconductor, as it quantifies the quantity and sign of the available charge carriers.

2.3 Experimental Theory

This experiment used a thin wafer of Indium Antimonide with an unknown doping. Attached to the wafer were four wired connections with one pair of wires carrying the primary driving current, I. The other pair were put through a voltmeter to measure the voltage, V_H, due to the Hall effect. The wafer was placed inside a magnetic field of known strength B.

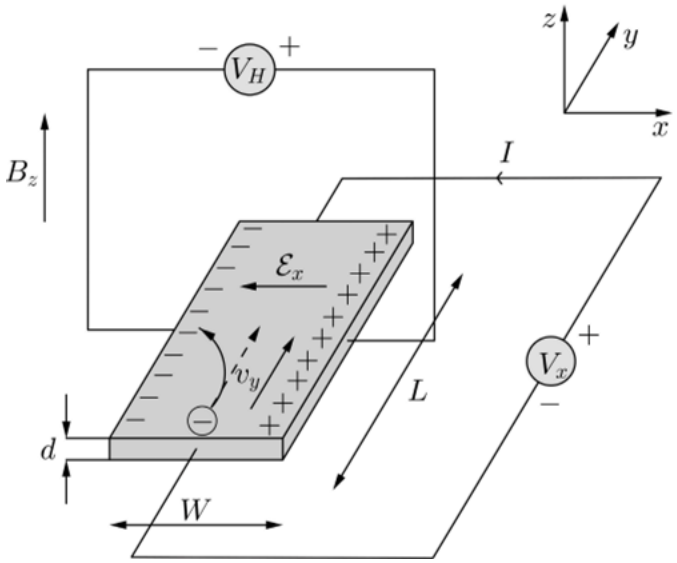

Figure 2.3: Diagram of the semiconductor wafer with attached circuitry.[4] This circuit is analogous to the one used in the experiment.

A description of the geometry, as shown in Figure 2.3, behind the motion of charge carriers inside the wafer, is essential to understanding the Hall effect in this experiment. The following equations make use of Figure 2.3 and assume that each element lies in either the xy or xz plane. In doing this, the vector equation can be simplified to only use the magnitudes of F_e, E, v and B.

The assumption is made that the magnetic field was perpendicular to the direction of current and the mean drift velocity of the electrons. It is worth noting that conventional current travels in the opposite direction to the flow of electrons, as is visible in Figure 2.3. The next step was to consider the force due to the magnetic and electric fields in the $-x$ direction, as shown in Equation (2.2.1), each as a separate force.

Firstly, the force on individual electrons due to the magnetic field is considered. Electrons are used as an example, but as will become clear, the type of the charge carrier is not important. The force is given by

$$F_m = ev_yB. \tag{2.3.1}$$

Where $e \approx 1.602 \times 10^{-19}$C, again, is the fundamental charge, v_y is the mean drift velocity of the electrons, opposite to conventional current I. Separately, the driving current across the wafer is given by

$$I = neAv_d. \tag{2.3.2}$$

Here, n is the number of charge carriers and $A = Wd$ is the cross-sectional area of the wafer, given by it's width, W, multiplied by its thickness, d. Rearranging for v_d and equating Equations (2.3.2) and (2.3.3) gives the force due to the magnetic field,

$$F_m = \frac{IB}{nA}. \tag{2.3.3}$$

In contrast, the electric component is trivial to derive from the definition of potential difference, $\Delta V = -Ed$, from Equation (2.2.1), it is simply qE. For the electron example, this equates to

$$F_e = \frac{eV_H}{d}. \tag{2.3.4}$$

The assumption is made that the circuit reaches a steady state near instantaneously. It's worth noting that a rising temperature due to any internal resistance will invalidate this assumption. This assumption means that the overall force is equal to zero and the magnitudes of both the magnetic and electric forces can be equated:

$$\frac{eV_H}{d} = \frac{IB}{nA}. \tag{2.3.5}$$

Re-arranging for the Hall voltage, V_H, allows the Hall coefficient to be extracted, R_H.

$$V_H = \frac{IBW}{neA} = \frac{IBW}{neWd} = \frac{IB}{ned} = R_H\frac{IB}{d}. \tag{2.3.6}$$

It is therefore possible, using the circuit setup in Figure 2.3, to determine the Hall coefficient for any semiconductor wafer. It's worth noting that R_H is not dependant upon the length, L, or width, W, of the wafer, only the thickness in the direction of the magnetic field, d. There are two key assumptions made in this theory which proved to be accurate for this experiment. Using a wafer of smaller width, or one with a larger internal resistance, may present systematic errors and these assumptions will need adjusting.

2.4 Isolating the Hall Voltage

For each increase in current, measurements were taken with the probe facing both perpendicular directions to the magnetic field. This gave us two Hall voltages per measurement of current. One voltage with the flat part of thickness d, facing towards the south pole of the magnet and the other towards the north pole, giving V_1 and V_2 respectively. Ideally $V_H = V_1 = V_2$, however, there is an absolute voltage drop over the wafer, V_R, due to its own internal resistance. Such that

$$V_1 = V_R \pm V_H, \tag{2.4.1}$$

$$V_2 = V_R \mp V_H, \tag{2.4.2}$$

depending on the orientation of the circuitry. These two equations can then be combined to eliminate V_R, this leaves only the desired Hall voltage, minus any residual voltage,

$$V_H = \frac{V_2 - V_1}{2}. \tag{2.4.3}$$

One added benefit of doing this is the reduction in error of the Hall voltage as it is effectively being measured twice per reading of current. The error on V_H can be determined from the errors on V_1 and V_2 as;

$$\Delta V_H = \sqrt{\frac{1}{4}(\Delta V_2^2 + \Delta V_1^2)}. \tag{2.4.4}$$

2.5 Expected Results

Rearranging Equation (2.3.6) gives an expression for the Hall coefficient in terms of Hall voltage, V_H, driving current, I, magnetic field strength, B and wafer thickness d;

$$R_H = \frac{dV_H}{IB}. \tag{2.5.1}$$

For this experiment, B and d were treated as constants where $B = (159 \pm 5)\text{mT}$ and $d = (1.50 \pm 0.01)\text{mm}$. This then makes current, I, the independent variable and V_H the dependant variable. Varying I and measuring V_H allowed the production of a graph of the form $y = mx$ by plotting V_H versus I. This

analysis shows that the expected relationship between the two variables is linear and passes through the origin. The gradient, m, is then given by three constants;

$$m = R_H \frac{B}{d} \Rightarrow R_H = \frac{md}{B}. \tag{2.5.2}$$

Dimensional analysis can be used to verify Equation (2.5.2), by converting the values into their derived SI units and then into true SI units, noting that R_H is the reciprocal of charge per volume;

$$R_H = \mathrm{mV}\frac{1}{\mathrm{A}}\frac{1}{\mathrm{T}} = \mathrm{m}\frac{\mathrm{kgm}^2}{\mathrm{s}^3\mathrm{A}}\frac{1}{\mathrm{A}}\frac{\mathrm{As}^2}{\mathrm{kg}} = \frac{\mathrm{m}^3}{\mathrm{As}} = \frac{\mathrm{m}^3}{\mathrm{C}} \tag{2.5.3}$$

as expected. The associated error on R_H can be given in terms of the error on m, d and B. The error on m is calculated by applying a least squares linear regression fitted to the measured values.

$$\Delta R_H = \sqrt{\left(\frac{\Delta md}{B}\right)^2 + \left(\frac{\Delta dm}{B}\right)^2 + \left(-\frac{\Delta Bmd}{B^2}\right)^2} \tag{2.5.4}$$

The expected outcome was to see a decrease in the value of the Hall coefficient with the decrease in temperature. This hypothesis was drawn from the band theory outlined in Section 2.1. The falling temperature means charge carriers of either type are less likely to be thermally excited into the conduction band and so their number and mobility would decrease.

3 Methodology

3.1 Equipment

- Two Voltmeters
- Power Supply with integrated Ammeter
- Borosilicate glass reciprocal, held in place by a clamp stand
- Dewar flask containing liquid nitrogen
- Indium Antimonide probe with four output wires
- A (black) wire to run from the ammeter to the voltmeter
- Protective eye-wear such as safety glasses suitable for use around liquid nitrogen

The equipment was kindly setup by a demonstrator prior to our arrival in the lab. A photograph of the apparatus is shown in Figure 3.1. The small, grey voltmeter was used to I to a greater degree of accuracy than the power supply would have been able to. The larger, red voltmeter was used to measure the Hall

voltages V_1 and V_2. The glass reciprocal was made from borosilicate glass due to it's low coefficient of thermal expansion of $\approx 5.16 \times 10^{-6}\text{K}^{-1}$.[5] This means it would not shatter due to thermal stress when liquid nitrogen was poured into it.

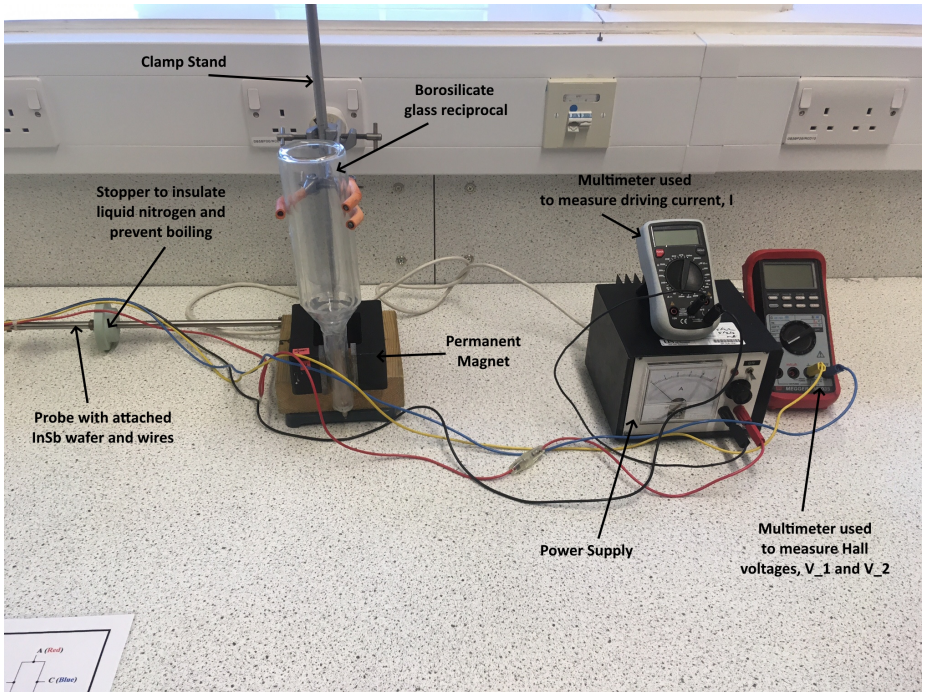

Figure 3.1: Photograph of the equipment setup prior to use in the experiment.

The probe consisted of a steal rod with the wafer and attached wires at one end. A rubber stopper on the probe meant the wafer was at the correct height when the probe was placed into the reciprocal. The rubber stopper also provided some insulation when liquid nitrogen was poured into the reciprocal, preventing it from boiling off and invalidating the assumed temperature of 77K.

3.2 Recording Data

When recording the data, significant care was taken not to exceed 20mA for extended periods of time. This would have led to an increase in the wafer temperature due to the I^2 term in the Joule-Lenz law; $P = I^2R$. A significant temperature increase across the wafer would have rendered both our temperature reading and the steady-state assumption invalid.

This meant readings were taken in quick succession. This was achieved by setting the current, measuring V_1, turning the probe 180 degrees and measuring V_2, before reducing the current back down to below 20mA. V_1 and V_2 were

set to be the south and north facing voltages respectively. It was important to be consistent for all the readings by using unambiguous visual indicators. To do this, we used the diagram on the reference card provided to us as the 'front-facing' side of the wafer, shown in Fig 3.2.

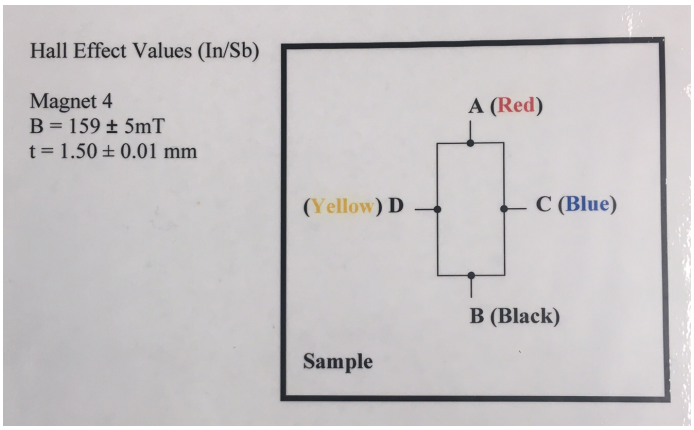

Figure 3.2: Card with data on the magnetic field strength, wafer thickness and the wire connections to the wafer. This was provided to us by the staff in the lab.

The errors for the first measurements of V_1 and V_2 were taken as ± 0.005mV for all values, whilst the errors for current were ± 0.5mA for all values except for the first reading which was ± 0.05mA. Otherwise, the results for the first readings at room temperature are shown in Table 2 below.

V_1 (mV)	V_2 (mV)	V_H (mV)	I (mA)
0.04	-0.02	-0.03	1.1
0.20	-0.12	-0.16	5.0
0.39	-0.25	-0.32	10.0
0.59	-0.38	-0.49	15.0
0.80	-0.50	-0.65	20.0
1.00	-0.61	-0.81	25.0
1.19	-0.77	-0.98	30.0
1.41	-0.90	-1.16	35.0
1.61	-1.02	-1.32	40.0
1.79	-1.14	-1.47	45.0

Table 2: Table of initial results for the experiment at 293K.

In order to take the readings at 77K, the probe was removed and the glass reciprocal was filled with liquid nitrogen from a larger Dewar flask. Whilst care should always be taken around cryogenic liquids anyway, it was paramount that the probe should be lowered back into the reciprocal very slowly. This was so

that the nitrogen would not boil violently due to the heat differential caused by the room temperature probe. Not only would nitrogen be lost, causing the sample to not be fully immersed, but it could also have boiled over and out of the reciprocal; a serious safety hazard. Otherwise, the procedure was the same as the first for this second set of results, shown in Table 3 below.

V_1 (mV)	V_2 (mV)	V_H (mV)	I (mA)
1.18	6.24	2.53	1.1
5.16	27.66	11.25	5.0
10.52	55.7	22.6	10.0
16.31	84.0	33.9	15.0
21.50	111.9	45.2	20.0
27.18	141.0	56.9	25.0
34.57	170.2	67.8	30.0
41.20	199.8	79.3	35.0
47.20	228.4	90.6	40.0
55.10	259.1	102.0	45.0

Table 3: Table of initial results for the experiment at 77K.

The primary difference in the second set of measurements is that there was a much higher variability in the readings of V_1 and V_2. The reading would frequently fluctuate and as such, the median value was taken for each reading. One hypothesis for this fluctuation is that any nitrogen conducting residual heat from the wafer boils. This was evident from the bubbles coming from the wafer after it was submerged for some time. It may have been the case that these bubbles interfere with the wafer's ability to consistently dissipate heat. This would cause the wafer's temperature, and thus resistivity, to fluctuate around, or slightly above, the 77K mark. This fluctuation was accounted for by increasing the errors taken for the voltage, which were taken as ± 0.25mV for all values of V_1 and the first two readings of V_2. The other readings of V_2 were given errors of ± 2.5mV due to the lower accuracy. The errors for current were the same as in the first set of readings.

4 Results and Analysis

4.1 Analysis of Recorded Data

For the analysis of the data, a Jupyter notebook running the Python programming language was used to manipulate the data and perform linear fits of the form $y = mx$ using a least-square regression. This was done by defining the linear fit as a function and optimising it using the SciPy module, specifically the scipy.optimize.curve_fit function. The function returns the coefficient m and its associated error. The code used to do this specific task is shown in Figure 4.1.

```python
def linear(x, m): ## linear function of the form y = mx
    y = m * x
    return y

dof = len(x) - 1 ## Degrees of freedom
m0=1             ## Initial guess for m
popt, pcov = optimize.curve_fit(linear, x, y, p0=m0, sigma=y_error)

m = popt[0]                     ## m from least squares regression
errors = np.sqrt(np.diag(pcov)) ## convert covariance matrix to error
m_err = errors[0]               ## error of m
y_fit = straight_line(x, m)     ## fitted values of y
```

Figure 4.1: Code snippet used to perform a linear fit of the variables y and x. For this experiment, y and x correspond to V_H and I respectively.

The residuals are then calculated natively in python, these show how the true values deviated from the proposed fit. From here, both the χ^2 and reduced χ^2 are calculated from the residuals, y errors and degrees of freedom.

```python
res = y - y_fit                         ## Residuals
chiSq = np.sum(res**2/y_error**2)       ## Chi-Squared value
rChiSq = chi_square/dof                 ## Reduced Chi-Squared = ChiSq / Degrees of Freedom
```

Figure 4.2: Code snippet used to calculate the χ^2 and reduced χ^2.

A p-value was also calculated from the χ^2 and the degrees of freedom. This is a measure of how well the data fits a model, the linear $y = mx$ one in this case.

```python
def pValue(chiSq, deg):                     ## Calculate p-value
    return special.gammaincc(deg/2, chiSq/2)  ## The incomplete gamma function from scipy.special
```

Figure 4.3: Function used to calculate the p-value coded natively in python. A p-value of approximately one was obtained for both sets of data.

The p-value was approximately one to at least five decimal places. This validates that the outlined theory is correct and the line of best fit passes through the origin. Practically this is a sound conclusion, as zero current would give zero Hall voltage, even with the rest of the apparatus, such as the magnet, unchanged.

4.2 Graphs for 291K

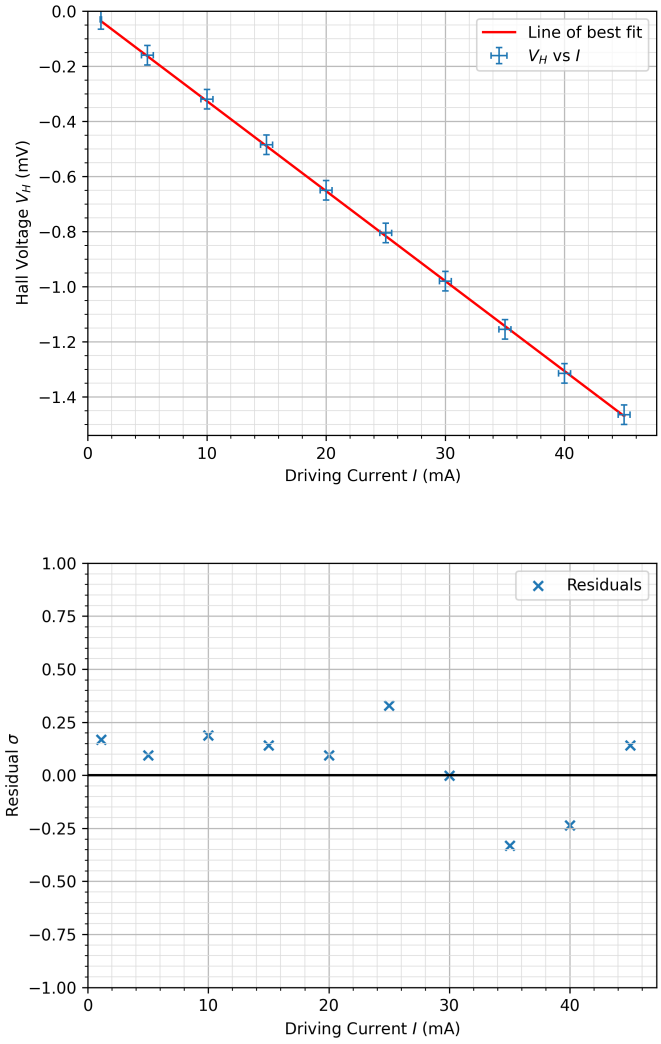

Figure 4.4: Graph of Hall voltage, V_H, versus driving current, I, with a linear best fit of the form $y = mx$. A graph of residuals is also included. This is for the data gathered at a temperature of 291K. The absolute value of the residuals are all less than one, which indicates the data conforms well to the model.

4.3 Graphs for 77K

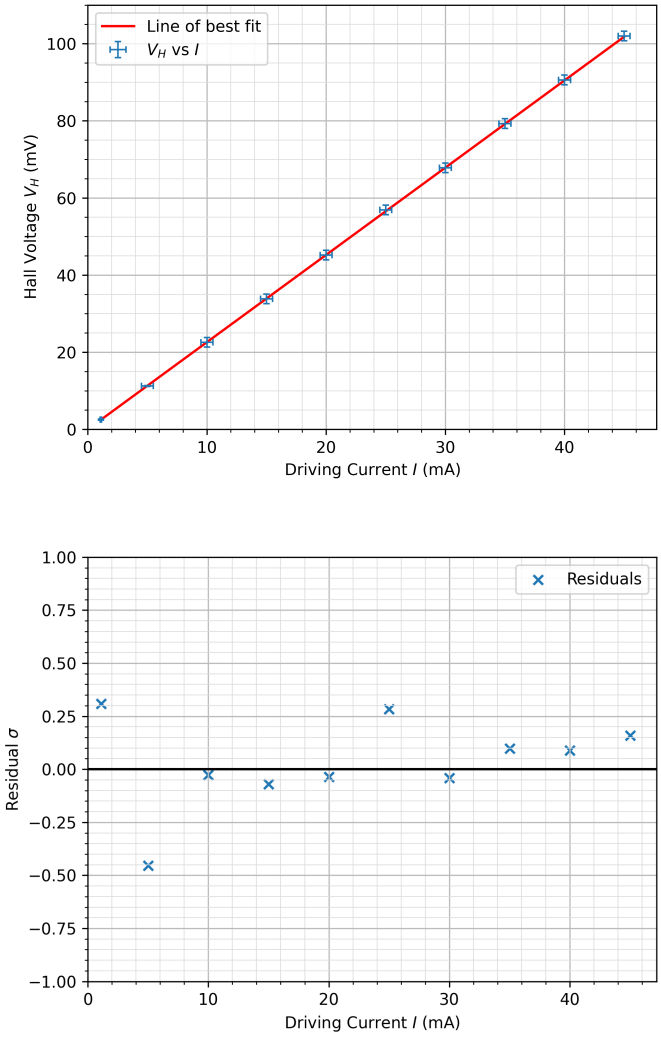

Figure 4.5: Graph of Hall voltage, V_H, versus driving current, I, with a linear best fit of the form $y = mx$. A graph of residuals is also included. This is for the data gathered at a temperature of 77K. The absolute value of the residuals are also all less than one.

4.4 Final Results

With the use of the aforementioned analysis, the Jupyter notebook calculated the final results after inputting our initial sets of data.

Temperature K	Hall Coefficient R_H	Reduced χ^2
291	$-(3.1 \pm 0.1) \times 10^{-4}$	0.044
77	$(2.13 \pm 0.07) \times 10^{-2}$	0.048

Table 1: Hall coefficient result for InSb at 293K and 77K.

The fluctuations in voltage for the second set of data was accounted for by increasing the errors of V_1 and V_2. Using the initial uncertainty due to the precision of the instruments still results in a $\chi^2 \approx 0.5$. It indicates that the data is an accurate description of the model and theory and that accounting for these fluctuations, whilst good practice, was not wholly necessary.

From the results obtained, it is clear that the Hall coefficient not only changes signs, but also increases in magnitude. This implies that mobility or number of negative charge carriers decreases relative to positive charge carriers. This is likely because, at a lower temperature, there is a reduction in the thermal excitation of electrons from the valence band to the conduction band. This reduces the mobility and availability of negative charge carries, changing the sign of R_H from negative to positive. This implies the semiconductor is n-type at room temperature, but changes to a p-type semiconductor at 77K.

5 Conclusion

The placement of and Indium Antimonide wafer in a constant magnetic field allows the accurate determination of the Hall coefficient at both room temperature and 77K. The method of determination is straightforward and easily repeatable with liquid nitrogen and readily available apparatus.

This study was only able to measure the Hall coefficient at two distinct temperatures, other experimental setups make use of heaters and calibrated thermistors to make continuous measurements of R_H with temperature.[6] Other research has found that this relationship is theoretically non-trivial for many semiconductors and requires experimental results to validate the relationship for real-world applications.[7]

The Hall effect can also be used to measure the Hall coefficient and other material properties of semiconductors, such as resistivity. These studies make use of the Van der Pauw method, it uses contacts at the corners of the wafer rather than the sides but is experimentally very similar to this method.[8]

Acknowledgements

I'd like to thank the teaching staff of the Year 2 Lab Module at the University of Sussex for giving me the opportunity and equipment to perform this experiment. I would also like to thank my lab partner Cauis Phillipo for his assistance during the experiment.

References

[1] David J. Griffiths, *Introduction to Electrodynamics*. p.247, Prentice Hall, Upper Saddle River, Third Edition, 1999.

[2] Nanoscale Device Characterization Division, Webpage, National Institute of Standards and Technology, US Department of Commerce, Last Accessed 05/01/2024. `https://www.nist.gov/pml/nanoscale-device-characterization-division/popular-links/hall-effect/hall-effect-measurements-3`

[3] Edward Ramsden *Hall-Effect Sensors: THeory and Application* Elsevier, First Edition, 2011.

[4] THE (CLASSICAL) HALL EFFECT, Webpage, Last Accessed 05/01/2024. `https://ebrary.net/158504/mathematics/classical_hall_effect`

[5] Soo-Jin Park, Min-Kang Seo, *Interface Science and Composites*, Interface Science and Technology, Section 6.3.3.1, 2011.

[6] Ivelina N. Cholakova, Member, IEEE, Tihomir B. Takov, Radostin Ts. Tsankov, Nicolas Simonne, *Temperature Influence on Hall Effect Sensors* 20th Telecommunications forum TELFOR 2012, 2012.

[7] S. K. Bansal, V. P. Duggal, *Temperature Dependence of Hall Coefficient and Electrical Resistivity in Sb Single Crystals at Low Temperatures Characteristics*, Physica Status Solidi, Volume 56, Issue 2, 1979.

[8] T. Hiraoka a, E. Kinoshita a, H. Tanaka b, T. Takabatake c, H. Fujii b *Hall effect and electrical resistivity in CeRhSb* Journal of Magnetism and Magnetic Materials, Volume 153, Issue 1-2, 1996.